Arp2/3 complex interactions and actin network turnover in lamellipodia

Frank PL Lai[1,7], Malgorzata Szczodrak[1,7], Jennifer Block[1], Jan Faix[2], Dennis Breitsprecher[2], Hans G Mannherz[3], Theresia EB Stradal[4], Graham A Dunn[5], J Victor Small[6] and Klemens Rottner[1,*]

[1]Cytoskeleton Dynamics Group, Helmholtz Centre for Infection Research, Braunschweig, Germany, [2]Institute for Biophysical Chemistry, Hannover Medical School, Hannover, Germany, [3]Department of Anatomy and Embryology, Ruhr University, Bochum, Germany, [4]Signalling and Motility Group, Helmholtz Centre for Infection Research, Braunschweig, Germany, [5]King's College London, Randall Division, New Hunt's House, London, UK and [6]Institute of Molecular Biotechnology, Austrian Academy of Sciences, Vienna, Austria

Cell migration is initiated by lamellipodia—membrane-enclosed sheets of cytoplasm containing densely packed actin filament networks. Although the molecular details of network turnover remain obscure, recent work points towards key roles in filament nucleation for Arp2/3 complex and its activator WAVE complex. Here, we combine fluorescence recovery after photobleaching (FRAP) of different lamellipodial components with a new method of data analysis to shed light on the dynamics of actin assembly/disassembly. We show that Arp2/3 complex is incorporated into the network exclusively at the lamellipodium tip, like actin, at sites coincident with WAVE complex accumulation. Capping protein likewise showed a turnover similar to actin and Arp2/3 complex, but was confined to the tip. In contrast, cortactin—another prominent Arp2/3 complex regulator—and ADF/cofilin—previously implicated in driving both filament nucleation and disassembly—were rapidly exchanged throughout the lamellipodium. These results suggest that Arp2/3- and WAVE complex-driven actin filament nucleation at the lamellipodium tip is uncoupled from the activities of both cortactin and cofilin. Network turnover is additionally regulated by the spatially segregated activities of capping protein at the tip and cofilin throughout the mesh.

*Corresponding author. Cytoskeleton Dynamics Group, Helmholtz Centre for Infection Research, Inhoffen Strasse 7, Braunschweig 38124, Germany. Tel.: +49 531 6181 3077; Fax: +49 531 6181 3099;
E-mail: klemens.rottner@helmholtz-hzi.de
[7]These authors contributed equally to this work

Introduction

The migration of cells and tissues is fundamental to metazoan life, driving tissue morphogenesis, homoeostasis and defence. Cell migration requires dynamic reorganization of the actin cytoskeleton, with filaments providing mechanical support of protrusion of the front and retraction of the rear. The lamellipodium, a thin leaflet of plasma membrane filled with actin filaments, constitutes the key organelle generating the force for directional protrusion of the cell periphery (Small *et al*, 2002; Pollard, 2007). Importantly, the actin filaments building the lamellipodium are oriented with their fast-growing, barbed ends pointing outwards (Small *et al*, 1978), allowing the centrifugal growth of the network. Work over the years has largely focused on signalling pathways stimulating the formation of these structures (Raftopoulou and Hall, 2004; Disanza *et al*, 2005), and the molecular players driving actin polymerization to induce and maintain them (Pollard and Borisy, 2003; Pollard, 2007). Although the increase in knowledge on the biochemical activities of factors implicated in actin polymerization at the cell periphery has been significant, the detailed actin assembly and disassembly kinetics in lamellipodia are unsettled and controversial. Breakthroughs in actin biochemistry include the discovery of the Arp2/3 complex (Machesky *et al*, 1994) and formins (Woychik *et al*, 1990), recognition of their relevance in nucleating actin filaments (reviewed in Goley and Welch, 2006; Goode and Eck, 2007; Pollard, 2007), as well as *in vitro* reconstitution of actin-based motility using purified proteins (Loisel *et al*, 1999; Romero *et al*, 2004). Spire (Quinlan *et al*, 2005) and Cordon-Bleu (Ahuja *et al*, 2007), implicated in vesicle trafficking and neuronal morphogenesis, respectively, add to the list of actin nucleators found in eukaryotes.

There is increasing consensus on the list of molecules harbouring key functions in lamellipodium protrusion (Small *et al*, 2002; Stradal and Scita, 2006), mostly based on manipulations of protein expression or activity. Suppression of Arp2/3 complex components by RNA interference (RNAi) or sequestration of the complex in the cytosol inhibits lamellipodia formation (Machesky and Insall, 1998; Kunda *et al*, 2003; Steffen *et al*, 2006). Arp2/3 complex activation in lamellipodia is thought to be mediated by WAVE complex (Stradal *et al*, 2004) and cortactin, although the relevance of cortactin in this process is controversial (Cosen-Binker and Kapus, 2006). Heterodimeric capping protein is also essential for Arp2/3 complex-mediated motility, both when reconstituted *in vitro* (Loisel *et al*, 1999) and *in vivo*, as RNAi-mediated knockdown causes excessive filopodia formation at the expense of lamellipodia (Mejillano *et al*, 2004). Another protein family of comparable relevance is ADF/cofilin proteins, which were proposed to promote lamellipodial protrusion by driving both actin

assembly and disassembly (Carlier *et al*, 1999; Ghosh *et al*, 2004; Hotulainen *et al*, 2005; Andrianantoandro and Pollard, 2006). All these factors are found to be enriched in lamellipodial protrusions, sometimes with significant spatial variations (Small *et al*, 2002), but their turnover rates in steady-state protrusion of live lamellipodia are much less well defined. For example, differences of opinion still exist about the site(s) of actin assembly within lamellipodia (Wang, 1985; Theriot and Mitchison, 1991; Small, 1995; Watanabe and Mitchison, 2002).

By employing state-of-the-art bleaching and photoactivation approaches combined with a new method of analysis and mathematical modelling, we revisit the mechanism of actin filament turnover in lamellipodia. Our findings, which reveal treadmilling for both actin and Arp2/3 complex, but uncoupling of their dynamics from cortactin and cofilin, call for a re-evaluation of the roles of these proteins in lamellipodia assembly.

Results and discussion

The turnover of lamellipodial actin was initially examined using fluorescence recovery after photobleaching (FRAP) (Wang, 1985) or photoactivation (Theriot and Mitchison, 1991), leading to the proposal of two distinct models for actin filament turnover in lamellipodia, treadmilling versus nucleation release, respectively. Whereas the former mechanism assumes assembly of individual lamellipodial filaments at the front and disassembly at the rear, the latter features short filaments, released from the front, and capable of continuous turnover throughout the lamellipodium (Small, 1995). Several groups have subsequently studied actin network flow using fluorescent speckle microscopy, which exploits inhomogeneous incorporation of low amounts of fluorescent molecules into polymer (Danuser and Waterman-Storer, 2006). Again, analysis of single-molecule speckles in lamellipodia suggested that most of the actin filaments in the lamellipodium are generated away from the tip by a mechanism now termed 'basal polymerization' (Watanabe and Mitchison, 2002), which is inconsistent, at least in part, with more recent studies (Hotulainen *et al*, 2005; Nakagawa *et al*, 2006; Iwasa and Mullins, 2007).

To re-evaluate when and where actin filaments are nucleated within lamellipodia of migrating cells, we bleached or photoactivated actin derivatives expressed in motile B16-F1 melanoma cells at various subcellular locations (Figure 1). In initial experiments, a laser scanning device of a confocal microscope was used to bleach rectangular regions in lamellipodia of cells expressing EGFP–actin, and recovery of fluorescence was recorded with wide-field imaging, enabling high spatial and temporal resolution (Figure 1A and Supplementary Movie 1). At 2 s after bleaching, a sharp rim of actin was observed at the lamellipodium tip, which progressively expanded rearwards into more proximal regions of the lamellipodium with an average speed of 3.78 μm/min (Figure 1A) ($n = 13$). These data already indicated a strong bias of incorporation of actin at the lamellipodium front, as observed previously (Wang, 1985), and are inconsistent with the view deduced from *in vitro* studies that treadmilling does not contribute much to actin filament turnover in cells (Pollard, 2007). To exclude the possibility that energy introduced into the system by bleaching may cause an experimentally induced modification of actin filament dynamics in our cells, we employed

two additional methods to study actin network turnover in lamellipodia: photoactivation and a pseudo-fluorescence loss in photobleaching (FLIP) approach. Activation of photoactivatable EGFP-tagged actin co-expressed with mRFP–actin revealed rapid rearward flow of the activated probe and its dissipation from the rear of the lamellipodium (Figure 1B), which largely coincided with exchange of non-activated actin from the front (see Supplementary Movie 2). Consistent with previous observations (Wang, 1985; Hotulainen *et al*, 2005; Nakagawa *et al*, 2006), these data supported a treadmilling mode of actin filament turnover in lamellipodia. However, it was recently proposed that FRAP and photoactivation of lamellipodial actin may lead to erroneous interpretations, due to significant turnover of the network from within the bleached or photoactivated area while flowing rearward (Watanabe and Mitchison, 2002). To exclude a contribution of intra-lamellipodial assembly/disassembly events to network turnover, we bleached thin lines parallel to the lamellipodial leading edge and established that the bleached lines travelled rearwards with the lamellipodial mesh (not shown) similar to wider bleached regions (see above). In addition, we exploited the rapid translocation of unpolymerized actin to the leading edge discovered recently (Zicha *et al*, 2003). In this FLIP type of experiment, we rapidly bleached the lamella in a position several microns behind the lamellipodium and recorded the incorporation of bleached actin monomers into the lamellipodial actin meshwork (Figure 1C and Supplementary Movie 3). Using photoactivation, the average speed of actin translocation to the leading edge was determined to be approximately $3.1 \pm 1.5\,\mu m/s$ in B16-F1 cells, with peak rates in individual cells of up to $6\,\mu m/s$ (data not shown). In the FLIP experiment, this rapid translocation of unpolymerized actin was detected as the incorporation of a narrow line of bleached actin into the lamellipodium tip (Figure 1C). If there were an active reorganization of the lamellipodial network by intra-lamellipodial assembly/disassembly (Watanabe and Mitchison, 2002), we would expect a rapid dissipation of the line of bleached actin, which was not the case. Instead, bleached actin from the lamella that incorporated into the lamellipodium tip flowed steadily rearwards in a well-defined line (Figure 1C), consistent with treadmilling.

A Monte Carlo model of diffusion was employed to simulate the fluorescence recovery observed in the lamellipodium shown in Figure 1A (for details on the model, see Supplementary data). The model that best fitted the experimental data is shown in Figure 1D (compare Figure 1A and D, see Supplementary Movie 4) and assumed actin assembly probability to be highest at the leading edge (for actin assembly and disassembly probability profiles relative to the distance from the leading edge, see Figure 1E). From these data, we conclude that actin predominantly polymerizes at the lamellipodium front, presumably at the interface between plasma membrane and the filament ends in the network abutting the membrane. However, to obtain a more unbiased determination of the dynamic behaviour of actin, applicable also to the regulatory molecules studied here, we developed a quantifiable parameter which we called 'treadmilling factor' (TMF) (Figure 1F, see Supplementary Movie 5). To obtain the TMF, we extracted and plotted the recovery of fluorescence in both the front and the rear half of the lamellipodium over time (Figure 1G). Upon normalization of
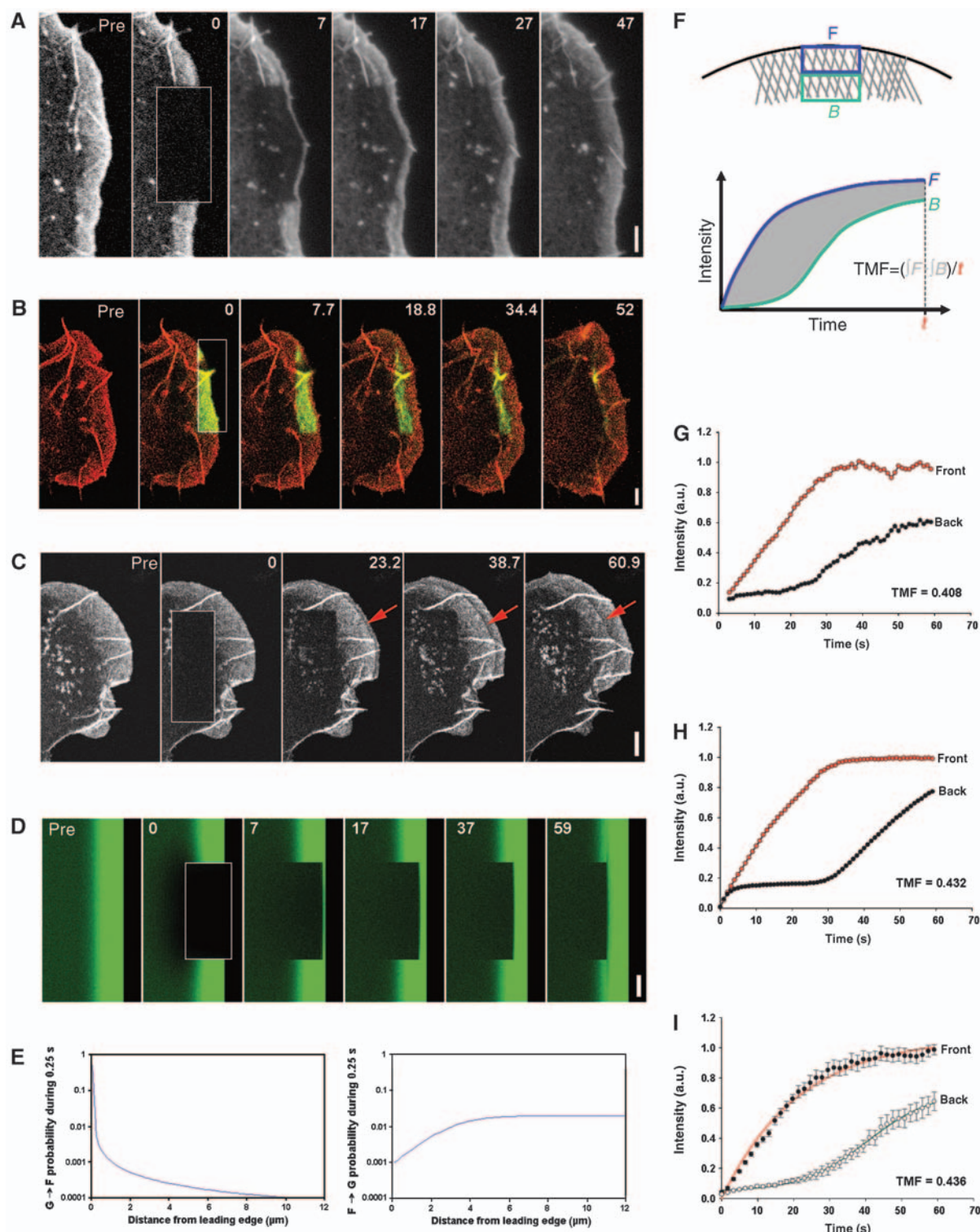
Figure 1 Actin assembly is restricted to the lamellipodium tip. (**A**) FRAP of EGFP–actin in lamellipodium of B16-F1 cell bleached as indicated by rectangle. Numbers in post-bleach images correspond to seconds. Bar: 3 μm. (**B**) Photoactivation of PA–EGFP–actin (green) within a lamellipodial region as indicated by rectangle in cell co-expressing mRFP–actin (red). Bar: 2 μm. (**C**) Rapid translocation to the leading edge of EGFP–actin bleached in the lamella (rectangle). Bleached actin incorporates at the leading edge and treadmills rearwards with the actin filament network (red arrows). Bar: 2 μm. (**D**) Monte Carlo diffusion model of the experiment shown in (A), with actin assembly/disassembly probability profiles shown in (**E**). Bar: 3 μm. (E) G-to-F (polymerization) and F-to-G (depolymerization) probability as a function of distance from the leading edge assumed for the simulation shown in (D). (**F**) Diagram explaining TMF calculation. Average intensities of front (F) and back (B) parts of the lamellipodium are plotted over time, and differential intensity per unit time calculated as shown. (**G, H**) Treadmilling analyses of the experiment shown in (A) and of its simulation shown in (D), respectively. (**I**) Treadmilling analysis for EGFP–actin as averaged from six independent movies. Data correspond to means and s.e.m. of front and back halves of analysed lamellipodia as indicated. Linear curves correspond to best fits of averaged data.

fluorescence to compare individual movies (see Materials and methods), the TMF was taken as the difference between the two curves averaged over time and constituted a direct measure of biased recovery from the front (Figure 1G). For the movie shown in Figure 1A, the TMF was 0.41 (Figure 1G), which compared closely to 0.43 (Figure 1H) obtained from the computer simulation depicted in Figure 1D. According to definition, the latter value comes close to the highest possible value for a TMF for a component with continuous recovery from the front, at least for the lamellipodium width given (see Supplementary data and below). In contrast, proteins with homogenous recovery over the entire lamellipodium will display TMFs close to 0. Importantly, the TMF for EGFP–actin (0.44) obtained from the average curves of six movies recorded with a double scan-headed confocal (see Supplementary Movie 6) was practically identical to the value observed in the simulation (Figure 1I). Taken together, these data show that actin assembly in the lamellipodia of these motile cells occurs exclusively at the front, with the actin filament arrays turning over by treadmilling. In addition, rapid severing and re-annealing of actin filaments as proposed recently to drive dynamic network rearrangements in lamellipodia (Miyoshi *et al*, 2006) cannot occur with significant frequency in the lamellipodia of B16-F1 (this study) and MTLn3 (see below) cells, as well as fibroblasts (Wang, 1985) or neuronal cells (Nakagawa *et al*, 2006), because such activities would preclude a strongly biased recovery from the front.

Having developed a system to record and analyse the spatial and temporal features of actin network turnover in B16-F1 lamellipodia, we turned to studying established regulators of lamellipodia protrusion; initially the actin filament nucleating Arp2/3 complex and its lamellipodial activators, the WAVE complex and cortactin. To ascertain reliable analysis of Arp2/3 complex dynamics, both C- and N-terminal fusions of all seven subunits of the complex were screened for proper incorporation into lamellipodia, as described previously (Rottner *et al*, 2006). Of these, the smallest subunits ArpC5 (also know as p16) and ArpC4 (p20) were selected for further analysis. In contrast to recent observations with fluorescent speckle microscopy, which indicated enrichment only in the distal two-thirds of the lamellipodium (Iwasa and Mullins, 2007), we observed EGFP-tagged Arp2/3 complex subunits to accumulate in the entire lamellipodium (Supplementary Figure 1), consistent with original immunolabelling data (Welch *et al*, 1997), although lamellipodia were on average narrower than in cells expressing EGFP–actin (see below). Arp2/3 complex is considered to amplify the generation of rapidly growing barbed ends by mediating the branching of daughter filaments off the barbed ends or sides of mother filaments. Although Arp2/3 complex could in principle be activated by multiple molecules in lamellipodia, the WAVE complex, which is known to accumulate at the tips of these structures (Steffen *et al*, 2004; Stradal *et al*, 2004), is currently considered most relevant for their formation. Previous analyses of Arp2/3 complex speckles indicated dynamics different from actin speckles (Watanabe and Mitchison, 2002), with a biased incorporation at the lamellipodium front (Miyoshi *et al*, 2006; Iwasa and Mullins, 2007). Irrespective of its activation, Arp2/3 complex may also be subject to rapid turnover in deeper lamellipodial regions, for example, upon network debranching and/or dissociation from actin, which may have previously been missed in

single-molecule speckle analyses (Iwasa and Mullins, 2007). To establish lamellipodial Arp2/3 complex dynamics, we performed FRAP experiments with cells expressing ArpC4 (not shown) or ArpC5 (Figure 2A–C). As shown in Figure 2A and B (see also Supplementary Movie 7), Arp2/3 complex largely recovered from the front, which would be consistent with its activation at the lamellipodium tip where the WAVE complex is localized (Steffen *et al*, 2004). Analysis of the representative cell in Figure 2A showed a significant difference between fluorescence recovery at the front and rear part of the lamellipodium (Figure 2B), which was confirmed by the average recovery behaviour of all cells analysed (Figure 2C). As expression of Arp2/3 complex subunits caused narrowing of the lamellipodium as compared with actin expressers and as the TMF is sensitive to changes in lamellipodium width (see Supplementary Figure 2A and B), we used the average lamellipodium width of ArpC5 expressers for determining the TMFs of both ArpC5 and actin (actin$_{narrow}$, termed n-actin in Figure 2D). Interestingly, the TMF obtained for actin$_{narrow}$ was even less (0.28) than that measured for ArpC5 (0.33; Figure 2D; see also Table I). Thus, these data confirm exclusive incorporation of Arp2/3 complex at the lamellipodium front and preclude Arp2/3 complex-mediated branching along filament sides in deeper regions of the lamellipodium and/or active capping/uncapping dynamics on filament pointed ends (Mullins *et al*, 1998).

Arp2/3 complex turns over in the lamellipodium tip region with a half-time of recovery ($t_{1/2}$) of 7.1 s, which is almost identical to actin ($t_{1/2} = 7.5$ s), as expected for components incorporated into the lamellipodium network by treadmilling. We next asked how this compares to the dynamics of the presumptive activator of Arp2/3 complex at the lamellipodium tip, the WAVE complex. Of its five constituents—the ubiquitous complex comprises Sra-1, Nap1, Abi-1, HSPC300 and WAVE2 (Gautreau *et al*, 2004)—Abl interacting proteins (Abi) were the first to be shown to accumulate at the tips of protruding lamellipodia and filopodia (Stradal *et al*, 2001). Bleaching of Abi-1 at the lamellipodium tip and analysis of its recovery revealed that Abi-1 shows a comparably slow turnover in this location (Figure 2E and F, and Supplementary Movie 8), with a $t_{1/2}$ almost double that of Arp2/3 complex (13.6 s). To examine whether Abi-1 dynamics indeed reports back on the turnover of the entire WAVE complex, we also studied the turnover of WAVE2. As WAVE overexpression is known to suppress the protrusion of spontaneous lamellipodia, FRAP experiments on reasonably bright cells had to be combined with stimulation of lamellipodia formation by aluminium fluoride (AlF$_4^-$) treatment (Hahne *et al*, 2001). Surprisingly, WAVE2 turnover appeared significantly accelerated ($t_{1/2} = 8.6$) as compared with Abi-1 (Figure 2G and H, and Supplementary Movie 9). The increased turnover was not due to AlF$_4^-$ treatment, as preliminary rates measured in low WAVE2 expressers without treatment was at least as fast (not shown). Comparable turnover rates ($t_{1/2} = 6.4$) on the membrane were recently also reported for the haematopoietic Nap1 isoform Hem-1 (Weiner *et al*, 2007). Collectively, these data suggest that Abi-1 dynamics at the lamellipodium tip does not correlate precisely with the dynamics of the WAVE complex. However, this does not necessarily indicate dissociations of WAVE and Abi from each other or from other WAVE complex constituents in the lamellipodium tip. Instead, the differential turnover rates may be explained by
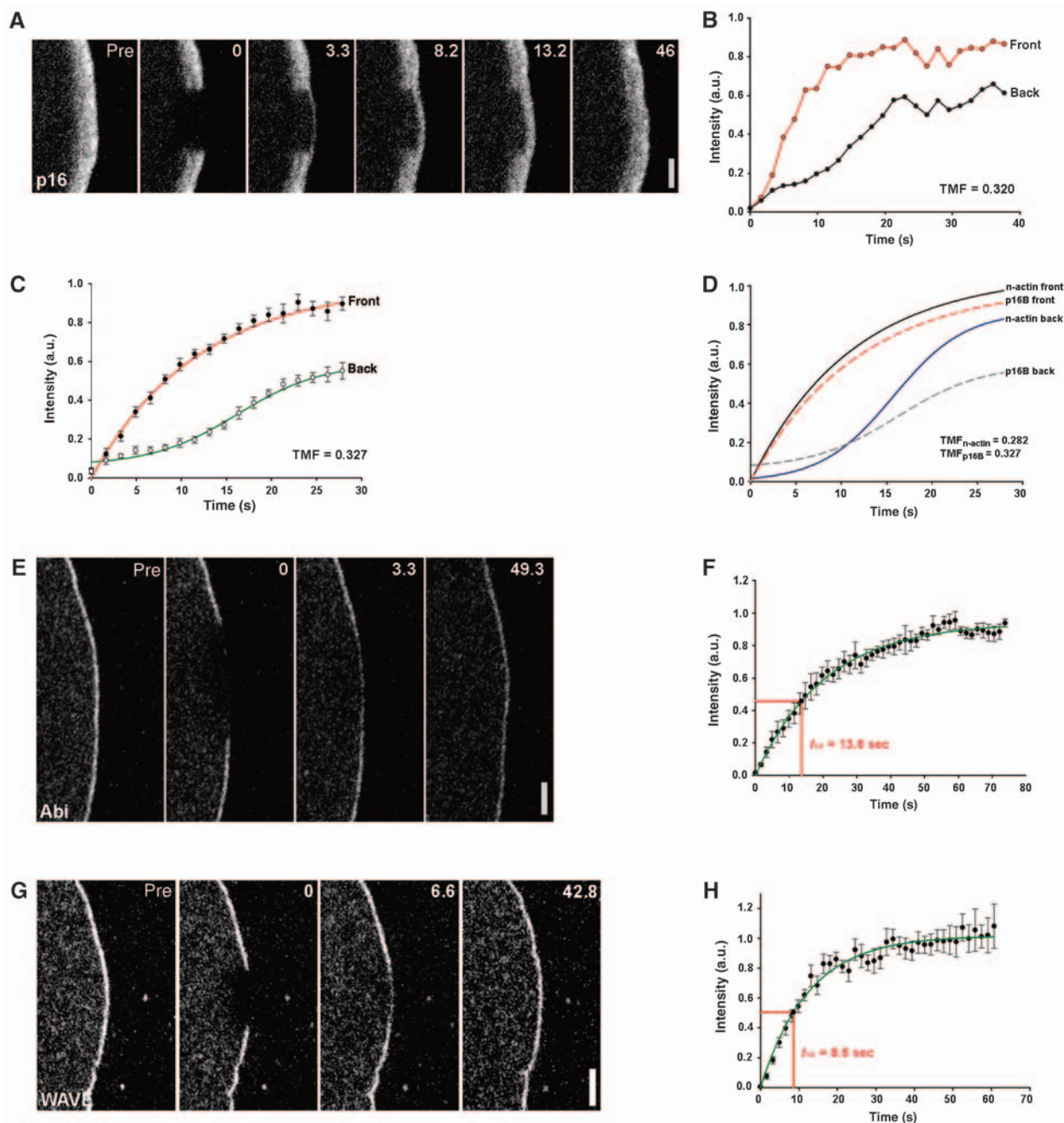
Figure 2 Arp2/3 complex dynamics as compared with WAVE and Abi. (**A**) FRAP of Arp2/3 complex (EGFP–ArpC5B) revealing its prominent incorporation at the lamellipodium tip. Time: seconds; bar: 2 μm. (**B**) Treadmilling analysis performed as depicted in Figure 1F for individual experiment shown in (A). (**C**) Results of EGFP–ArpC5B treadmilling analysis (means and s.e.m. from six independent movies) and best fits of averaged data as indicated. (**D**) Comparison of ArpC5B and actin analyses, with sizes of analysed lamellipodial areas set to the average lamellipodium width observed upon ArpC5B expression (n-actin designates actin$_{narrow}$, see also main text). Displayed are best fits of means (linear and dashed lines for actin and ArpC5B, respectively) of at least four movies for each component. (**E**) FRAP of the WAVE complex component Abi-1 at the lamellipodium tip. Bar: 2 μm. (**F**) Analysis of Abi-1 fluorescence recovery. Data are means and s.e.m. of five movies. Half-time of fluorescence recovery ($t_{1/2}$) was calculated from best linear fit (green curve). (**G**) FRAP of EGFP–WAVE2. Bar: 2 μm. (**H**) Analysis of WAVE2 fluorescence recovery. Data are means and s.e.m. of seven movies. Half-time of fluorescence recovery ($t_{1/2}$) was calculated from best linear fit (green curve).

the fact that Abi-1 is able to engage in actin regulatory complexes additional to WAVE complex (Stradal and Scita, 2006). Thus, individual Abi molecules may be retained in the lamellipodium tip by these additional interactions, for instance with Eps8 or Ena/VASP proteins (Tani *et al*, 2003). This would be consistent with the similar turnover rates ($t_{1/2}=14.4$ s) observed for the Ena/VASP family member

VASP (Supplementary Figure 3 and Movie 10). Notwithstanding this, Arp2/3 complex turnover at the lamellipodium is worthwhile to be compared with that of its activator WAVE. Although the half-times of fluorescence recovery in the tip region of the lamellipodium are comparable for WAVE and Arp2/3 complex (see also Table I), they are not inconsistent with multiple Arp2/3 complex activations executed by

individual WAVE complex units, in analogy to what is known for Arp2/3 complex activators retained at bacterial or bead surfaces (Wiesner *et al*, 2003; Carlier and Pantaloni, 2007; Pollard, 2007). However, prerequisites for this assumption to hold true are as follows: the observed fluorescence intensities of Arp2/3 complex and WAVE reflect comparable amounts of endogenous complexes present, and the actual zone of Arp2/3 complex activation at the membrane, corresponding

Table I Summary of treadmilling factors (TMFs) and half-times of fluorescence recovery ($t_{1/2}$) measured in this study

Component	TMF	$t_{1/2}$
Actin	0.436	21.3
p16	0.327	9.2
Actin$_{narrow}$	0.282	11.1
Actin$_{tip}$	—	7.5
p16$_{tip}$	—	7.1
Abi	—	13.6
WAVE	—	8.6
Cttn	0.155	6.4
Cttn II	0.159	3.8
CP	—	7.2
Cofilin	0.061	6.5
Cofilin$_{active}$	0.076	4.2
Cofilin$_{inactive}$	0.066	2.8
VASP	—	14.4

Actin$_{narrow}$ (also termed n-actin in Figure 2) corresponds to values obtained from actin movies measured as done for p16 expressers. The average width of measured areas in p16 expressors was approximately 1 μm, whereas the tip measurements were done on regions with a dimension of approximately 0.5 μm. The average width analysed in lamellipodia of actin expressers was 2.8 μm.
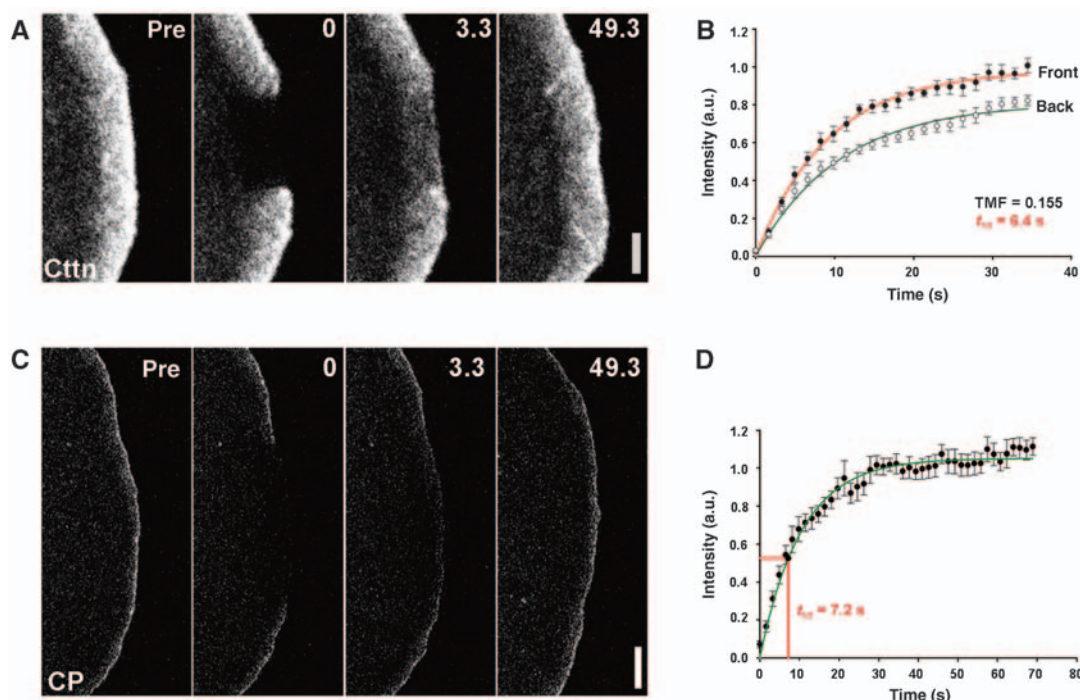
to WAVE localization, is much more restricted than what we define as the tip region by light microscopy, which is likely. In any case, our data also suggest that WAVE, Abi and VASP are components of perhaps partially associated, larger protein assemblies, which share the feature of being pushed forward by the network of polymerizing actin filaments they are engaged in regulating.

The second Arp2/3 complex activator enriched in lamellipodia is the type II nucleation-promoting factor cortactin (Cosen-Binker and Kapus, 2006). In contrast to WAVE (Figure 2G), cortactin labels the entire lamellipodium (Figure 3A and Supplementary Figure 4A and C), in a manner indistinguishable from Arp2/3 complex (Figure 2A, see also Supplementary Figure 1). Nevertheless, its dynamics in the lamellipodium significantly differed from that of actin and Arp2/3 (Supplementary Movies 11–13). First, cortactin did not recover in a treadmilling manner as observed for actin or the Arp2/3 complex (cortactin TMFs = 0.15 and 0.16 for two independent constructs, respectively; Figure 3B and Supplementary Figure 4B). We conclude that the slight deviation from 0 was largely due to the density gradient of cortactin localization from distal to more proximal lamellipodial regions (Figure 3A), which tightly follows that of actin (Rottner *et al*, 1999; Small *et al*, 2002), and not due to partial treadmilling. This view was corroborated by the best linear fit for the rear-half recovery curve, which was exponential for both cortactin constructs (Figure 3B and Supplementary Figure 4B), and not sigmoidal as observed for treadmilling components such as actin and Arp2/3 complex (Figures 1E and 2C). Second, the turnover of cortactin in the lamellipo-

Figure 3 Turnover of cortactin and capping protein in the lamellipodium. (**A**) FRAP of EGFP–cortactin (construct 1) as indicated. Time: seconds; bar: 2 μm. (**B**) Treadmilling analysis of EGFP–cortactin. Plotted are averaged data (means and s.e.m. of means) and best linear fits of six independent movies. The comparably low TMF is due to homogenous fluorescence recovery in the entire lamellipodium. $t_{1/2}$ given was calculated for entire lamellipodium. (**C**) FRAP of EGFP-tagged CP-beta2, the accumulation of which is largely confined to the lamellipodium front (see also Supplementary Figure 5). Bar: 2 μm. (**D**) Summary of FRAP analysis for CP-beta2. Data are means and s.e.m. (eight movies) as well as best linear fit (green) of averaged data. $t_{1/2}$ of fluorescence recovery was calculated from best linear fit.

dium was comparably fast, albeit with moderately divergent recovery times measured for the two constructs ($t_{1/2} = 6.4$ and 3.8 s; compare with $t_{1/2}$ of actin in the entire lamellipodium $= 21.3$ s; see also Table I). To exclude that the two different EGFP–cortactin constructs used did not display erroneous behaviour perhaps due to being non-functional, we tested a third, independently generated EGFP–cortactin, the functionality of which had previously been confirmed by reconstitution of a knockdown phenotype (Zhu *et al*, 2007). Not unexpectedly, this cortactin variant again displayed rapid, and continuous recovery throughout the entire lamellipodium, without convincing bias of recovery from the front (Supplementary Figure 4C and Supplementary Movie 13), revealing that cortactin recovery does not follow the treadmilling behaviour in lamellipodia as observed for actin and Arp2/3 complex. Thus, although the mechanistic subtleties of cortactin function in lamellipodia remain unclear, the dynamics of most cortactin molecules, at least in deeper lamellipodial regions, is inconsistent with their engagement in the promotion of Arp2/3 complex activation. Through its ability to interact with both F-actin and the Arp2/3 complex (Cosen-Binker and Kapus, 2006), cortactin may serve to stabilize Arp2/3 complex-induced actin networks rather than drive their (Arp2/3-mediated) assembly.

Two other lamellipodial proteins are considered indispensable for proper lamellipodium protrusion and Arp2/3-mediated motility in general (Carlier and Pantaloni, 2007): heterodimeric capping protein (Mejillano *et al*, 2004) and ADF/cofilin (Kiuchi *et al*, 2007). Similar to previous observations (Mejillano *et al*, 2004; Iwasa and Mullins, 2007), we found capping protein enriched in the front region of the lamellipodium (Supplementary Figure 5), and FRAP experiments revealed a $t_{1/2}$ of recovery at the lamellipodium tip of approximately 7.2 s (Figure 3C and D, and Supplementary Movie 14), almost an order of magnitude slower than deduced from speckle analysis (Miyoshi *et al*, 2006). The reason for this discrepancy is unclear, but could arise from the difficulty to ascertain speckle dynamics for proteins with tight spatial restriction, like capping protein (Figure 3C), WAVE complex components or VASP. For example, fluorescent speckle analysis in the same study indicated EGFP–VASP not to display any continuous association with the lamellipodium tip (Miyoshi *et al*, 2006), whereas FRAP experiments revealed quite slow turnover in this location (Applewhite *et al*, 2007) (see also Supplementary Figure 2, Supplementary Movie 10 and Table I). Assuming a balance of actin assembly and disassembly in the lamellipodium at steady state, similar turnover rates at the lamellipodium tip for actin ($t_{1/2}$ of approximately 7.5 s) and capping protein ($t_{1/2} = 7.2$ s) indicate that capping protein does not dissociate from individual filaments until they are disassembled. This is probable at least for filaments short enough to be disassembled within the observed time frame. The dependence of capping protein accumulation in the tip region on actin filaments is corroborated by its loss upon filament depolymerization by latrunculin B (Supplementary Figure 6 and Supplementary Movie 15). Furthermore, the restriction of capping protein to the front is inconsistent with significant retrograde flow of capped filaments into the lamellipodium mesh. As the absence of actin assembly behind the tip region as observed here precludes the existence of elongating barbed ends throughout the lamellipodium (see above),

maintenance of capping behind the tip region (if it exists) may be accomplished by additional factors. Potential candidates include Eps8 or twinfilin (Carlier and Pantaloni, 2007), although it should be noted that none of these factors are capable apparently of compensating for an essential aspect of capping protein function in lamellipodium protrusion revealed by RNAi (Mejillano *et al*, 2004). An alternative explanation of the data is that heterodimeric capping protein selectively aborts growth of short, non-productive filaments, perhaps subtending non-productive angles to the protruding lamellipodium front. Future work is required to test this possibility.

On the basis of *in vivo* and *in vitro* observations, ADF/cofilin is considered to enhance actin treadmilling by promoting both filament disassembly (Loisel *et al*, 1999; Kiuchi *et al*, 2007) and assembly (Ghosh *et al*, 2004; Andrianantoandro and Pollard, 2006). Interestingly, Kiuchi *et al* (2007) concluded that ADF/cofilin supports protrusion by maintaining a high actin monomer pool instead of driving nucleation, but they did not examine cofilin dynamics in the lamellipodium. We show here that cofilin, which readily associates with the entire lamellipodium (Figure 4A and Supplementary Movie 16), shows FRAP dynamics markedly different from actin or Arp2/3 complex, with a TMF of 0.061, and a $t_{1/2}$ for the entire lamellipodium of 6.5 s (Figure 4A and B). To exclude that ectopically expressed EGFP-tagged cofilin is subject to rapid inactivation by phosphorylation on serine 3 (Kiuchi *et al*, 2007), with the potential to change its dynamics, we also examined the turnover of a non-phosphorylatable constitutively active mutant (S3A) and an inactive, phosphorylation-mimetic cofilin (S3D). Interestingly, both mutants (Figure 4E, and Supplementary Movies 17 and 18) recovered throughout the entire lamellipodium with even faster turnover rates than wild-type cofilin (Figure 4E), indicating that phosphorylation/dephosphorylation events may retain the protein in the lamellipodium, but the TMF was virtually identical to the wild-type protein (see also Table I). These data show that inactivation (by phosphorylation) cannot have caused erratic behaviour of our wild-type cofilin. To prove that EGFP tagging had not generally abrogated the functionality of our cofilin, its activity was examined by a number of additional approaches. First, purified, EGFP-tagged cofilin quenched the fluorescence of pyrenylated actin filaments in a manner indistinguishable from untagged cofilin (Andrianantoandro and Pollard, 2006), demonstrating actin filament binding *in vitro* (Figure 4C). In addition, co-immunoprecipitations showed interaction of all expressed EGFP-tagged cofilin variants with actin in cell extracts, although, as expected, with less efficiency for the inactive variant (Supplementary Figure 7). Furthermore, filament depolymerization/severing mediated by EGFP-tagged wild-type cofilin was demonstrated both by co-sedimentation assay (Figure 4D) and by direct observation of fragmentation of individual actin filaments by total internal reflection fluorescence (TIRF) microscopy (Supplementary Figure 8). Thus, no indication was obtained to suggest that EGFP tagging abrogated the function of the cofilin variants used here, neither *in vivo* nor *in vitro*. Importantly, and as opposed to previous suggestions (Ghosh *et al*, 2004), comparison of actin and cofilin dynamics in lamellipodia thus precludes a significant role for cofilin in promoting nucleation, at least in B16-F1 cells. Instead, our data are consistent with cofilin
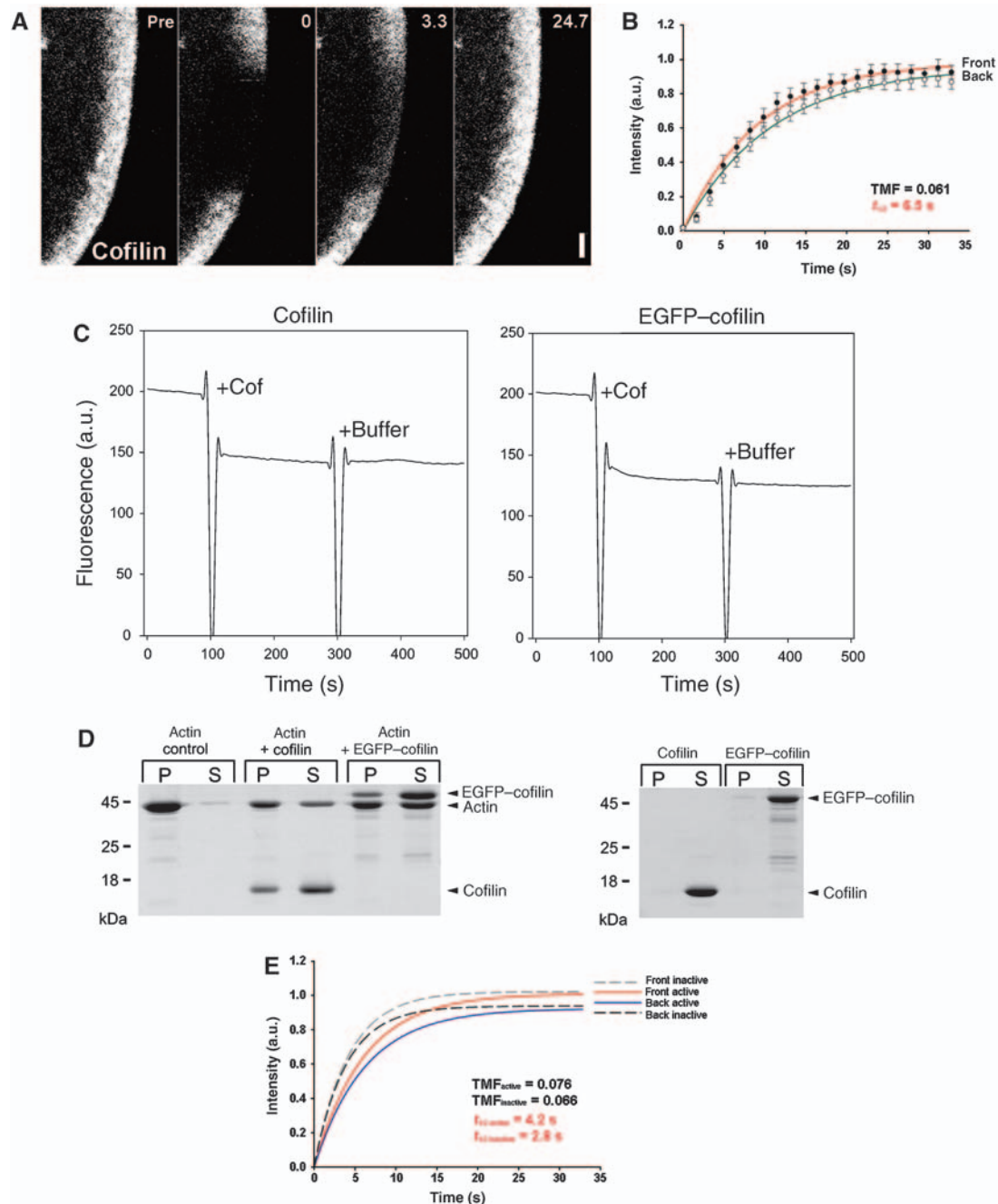
Figure 4 Characterization of cofilin turnover in B16-F1 cells. (**A**) FRAP of EGFP-tagged cofilin wild type as indicated. Time: seconds; bar: 2 μm. (**B**) Summary of treadmilling analysis for wild-type cofilin. Data are means and s.e.m. of five independent movies as well as linear fits of averaged data for front and back halves of the lamellipodium as indicated. Virtually no difference in fluorescence recovery between front and back lamellipodial halves was observed (TMF = 0.061). $t_{1/2}$ was calculated for entire lamellipodium. (**C**) Quenching of pyrenyl fluorescence by cofilin. Polymerized actin containing 10% pyrenyl-actin was diluted to 3 μM in a final volume of 1 ml, and after 100 s either 1 μM cofilin (left) or 1 μM EGFP–cofilin (right) were added (10 μl each) as indicated. After 200 s, 10 μl of 1 × actin polymerization buffer was added to the samples. The addition of both EGFP-tagged and untagged cofilin resulted in considerable quenching of pyrenyl fluorescence due to actin filament side binding, whereas buffer addition had no effect. (**D**) EGFP-tagged cofilin binds and depolymerizes actin filaments. (Left) 3 μM of polymerized actin was incubated with either 3 μM cofilin or 3 μM EGFP–cofilin for 2 h at 21°C. After high-speed sedimentation, proteins from pellets (P) and supernatants (S) were analysed by SDS–PAGE and Coomassie blue staining. Both cofilins are able to bind actin filaments as revealed by their appearance in the pellets (P), and their presence causes a considerable amount of actin to shift to the supernatant (S) fractions. Thus, in addition to binding, both cofilin variants promote actin filament disassembly in an indistinguishable manner. (Right) Neither cofilin variant is found in the pellet fraction in the absence of actin. (**E**) Best linear fits of averaged data from treadmilling analyses performed on FRAP movies acquired as shown in (A) of active (solid lines) and inactive (dashed lines) cofilin mutants as indicated (at least three movies for each mutant). Respective $t_{1/2}$ values were calculated for the entire lamellipodium.

supporting protrusion indirectly by promoting F-actin disassembly both in lamellipodia and other cellular locations (Kiuchi *et al*, 2007). Finally, to confirm the general relevance

of this observation, we extended our experimental approach to MTLn3 mammary carcinoma cells, which are frequently used to study cofilin function *in vivo* (Ghosh *et al*, 2004; van

Rheenen *et al*, 2007). MTLn3 cells expressing EGFP–actin or cofilin were induced to form lamellipodia with EGF and subjected to FRAP analysis as described above (Figure 5 and Supplementary Movies 19 and 20). Interestingly, the actin network in lamellipodia stimulated by EGF also turned

over by treadmilling, whereas cofilin did not, indistinguishable from the observations made with B16-F1 cells moving on laminin.

Collectively, from previous work and the data presented here, we provide a comprehensive model of steady-state lamellipodium protrusion (Figure 6), in which Arp2/3-mediated birth of filaments at the lamellipodium tip—activated by WAVE complex—is counterbalanced by capping of unproductive filaments at the tip and actin disassembly from the rear. In this scenario, neither cortactin nor cofilin is engaged in nucleation (Ghosh *et al*, 2004; Andrianantoandro and Pollard, 2006; Cosen-Binker and Kapus, 2006) or severing and re-annealing, as proposed for cofilin recently (Miyoshi *et al*, 2006). Our findings call for a revision of ideas about lamellipodia turnover (Watanabe and Mitchison, 2002) and the role of cortactin in actin-based motile processes.

Figure 5 Actin and cofilin turnover in MTLn3 cells. FRAP of EGFP–actin (**A**) or EGFP–cofilin (**B**) in lamellipodia of MTLn3 cells shortly after EGF treatment (5 nM). Time: seconds; bars: 5 μm. Note exclusive recovery of actin but not cofilin from the front.

Materials and methods

DNA constructs and protein purification
The DNA constructs used here are listed in Supplementary data. GST-tagged cofilin constructs were expressed in *Escherichia coli* strain Rossetta (Promega) and purified from bacterial extracts on glutathione-conjugated agarose (Sigma-Aldrich, Germany) using
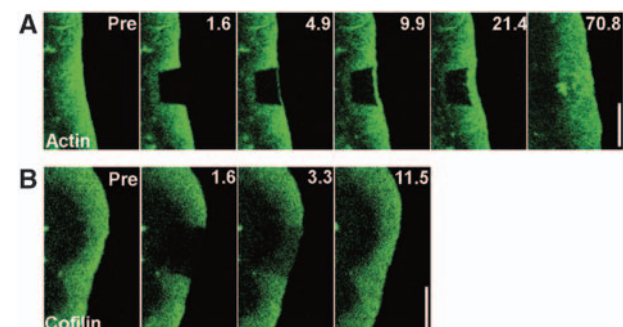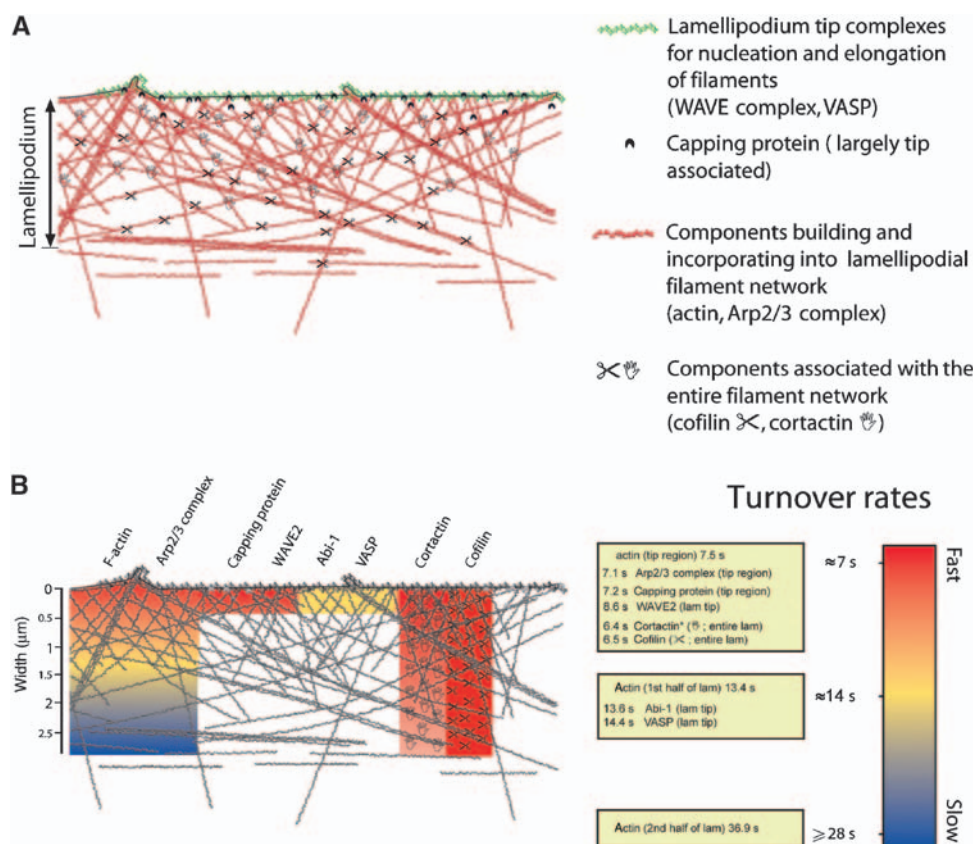

Figure 6 Schematic model summarizing the major results obtained in this study. (**A**) The lamellipodium is built by components, which fall into different categories. Here, we distinguish four of those categories, based on their localization pattern within the lamellipodial structure, their dynamics and/or function: tip components driving actin assembly from the barbed end (WAVE complex components or VASP); capping protein, also largely associating with the tip; components incorporating into and building the network (actin and Arp2/3 complex), clearly displaying treadmilling behaviour; and factors associating with the entire lamellipodium (cofilin and cortactin) without treadmilling. (**B**) Summary of the turnover rates measured for these lamellipodial regulators as indicated. Colour code is displayed on the right. Note that for components with biased recovery from the lamellipodium tip (actin and Arp2/3 complex), recovery times differ dependent on the distance from the distal tip. For cortactin, the gradual decrease in colour intensity indicates the decrease in fluorescence intensity from front to rear of the lamellipodium observed for this component, but not for cofilin. Cream-coloured boxes summarize turnover rates (expressed as half-times of recovery of fluorescence intensity) as measured for different components in different intra-lamellipodial regions. *Value measured for the cortactin–EGFP construct used in Figure 3.

standard procedures. The GST tags were cleaved by incubating the purified fusion proteins with PreScission protease in phosphate-buffered saline (PBS), pH 7.3, supplemented with 1 mM dithiothreitol (DTT) and 1 mM EDTA overnight at 4°C. After cleavage, the GST tags were removed by passing the protein solution over glutathione-conjugated agarose columns. Cofilin and EGFP–cofilin remained in the flow through and were subsequently dialysed against PBS containing 1 mM DTT and 5 mM benzamidine. Protein concentrations were calculated from the predicted extinction coefficients (Invitrogen; Vector NTI software). Actin was purified from rabbit skeletal muscle as described (Spudich and Watt, 1971) and subsequently gel filtered on a Superdex 200 column using an ÄKTA purifier system (Amersham Pharmacia Biotech).

F-actin co-sedimentation and pyrene assays
For high-speed actin sedimentation assays, G-actin was first polymerized in actin polymerization buffer containing 10 mM imidazole, 2 mM $MgCl_2$, 0.2 mM $CaCl_2$, 1 mM Na-ATP, 1 mM DTT and 50 mM KCl, pH 7.2 for 2 h at 21°C. Subsequently, filamentous actin was incubated in actin polymerization buffer either in the presence or absence of untagged or GFP-tagged cofilin for additional 2 h at 21°C. The protein mixtures were then sedimented at 100 000 g in a Beckman Optima table top ultracentrifuge for 30 min, and the pellets brought to the original volume in SDS sample buffer. Pellet and supernatant fractions were analysed by SDS–PAGE and Coomassie blue staining.

Quenching of pyrenyl fluorescence by cofilin was determined by fluorescence spectroscopy on a Jasco FP-6500 spectrofluorometer at 343 nm excitation wavelength and 384 nm emission wavelength. Briefly, 3 μM F-actin (10% pyrenyl labeled) in actin polymerization buffer was measured alone or after the addition of either untagged or GFP-tagged cofilin (1 μM each) at 21°C.

Cells, transfections and immunoprecipitations
Mouse melanoma cells (B16-F1) were from American Type Culture Collection (ATCC CRL-6323) and maintained in DMEM (Invitrogen, Germany) with 10% FCS (PAA Laboratories, Austria) at 37°C in the presence of 5% CO_2. MTLn3 cells, kindly provided by Jeff Segall and Bob van de Water, were maintained in DMEM, 5% FBS (Sigma) and 2 mM glutamine. Cells were transfected using Superfect (Invitrogen) and Fugene HD (Roche) for B16-F1 and MTLn3, respectively. Following transfection, B16-F1 cells were plated in Ham's F12 medium (Sigma-Aldrich) containing 10% FCS onto acid-washed glass coverslips coated with 25 μg/ml laminin (Sigma-Aldrich), and examined on the same day. Aluminium fluoride treatment was carried out as described (Steffen *et al*, 2004). MTLn3 cells were seeded on glass overnight and stimulated with EGF (5 nM) shortly before movie acquisition.

FRAP
Cells were observed in an open, heated chamber (Warner Instruments, Reading, UK) at 37°C on inverted microscopes. FRAP experiments were performed by utilizing different scanning confocal microscope systems. Initial experiments as the one shown in Figure 1A were performed on a LSM 510 Meta (Zeiss, Jena, Germany), which was equipped with a 100 ×, 1.45NA αPlan-FLUAR TIRF objective (Zeiss) and an interline transfer, progressive scan CCD camera (Coolsnap$_{HQ}$; Photometrics, Tucson, AZ, USA) driven by Metamorph software (Molecular Devices Corp., Downingtown, PA, USA). Selected cellular areas covering parts of protruding lamellipodia were bleached (30 iterations at full laser power at 488 nm, 30 mW argon laser) immediately after and before one full-frame scan of respective fields, which was followed by switching to epi-fluorescence imaging using a mercury lamp (100 W) as light source. Switching time was approximately 2 s.

The majority of experiments was performed using a double-scan-headed confocal microscope (Fluoview1000, Olympus), allowing simultaneous imaging of EGFP- and/or RFP-tagged probes (with 30 mW 488 nm multiline argon and/or 20 mW 561 nm solid-state lasers, respectively) and photobleaching/activation using a 20 mW 405 nm diode laser. Circular regions and rectangles were bleached/photoactivated in the tornado and regular line-scanning modes, respectively. Output laser powers were approximately 5–10% for photobleaching and <5% for photoactivation. EGFP and mRFP imaging was carried out at laser powers of approximately 1–5 and 10–20%, respectively. A 100 × /1.45NA PlanApo TIRF objective (Olympus Inc.) was used in all experiments. Most movies were acquired at a scanning rate of 1.644 s per frame. Image analysis was carried out on a PC using FV10-ASW 1.6 viewer (Olympus Inc., Olympus, Hamburg, Germany), ImageJ (http://rsb.info.nih.gov/ij/), Metamorph (Molecular Devices Corp.) and Adobe Photoshop CS software.

FRAP data were analysed as described in Supplementary data, using SigmaPlot 10.0 (Scientific Solutions SA, Pully-Lausanne, Switzerland) and Microsoft Excel 2000. The diagrams shown in Figures 1F and 6 were drawn using Microsoft Powerpoint 2000 and Adobe Illustrator CS2, respectively. The simulations of actin recovery in the lamellipodium were carried out as detailed in the Supplementary data and using Mathematica version 5.2.

Supplementary data
Supplementary data are available at *The EMBO Journal* Online (http://www.embojournal.org).

References

Ahuja R, Pinyol R, Reichenbach N, Custer L, Klingensmith J, Kessels MM, Qualmann B (2007) Cordon-bleu is an actin nucleation factor and controls neuronal morphology. *Cell* **131:** 337–350

Andrianantoandro E, Pollard TD (2006) Mechanism of actin filament turnover by severing and nucleation at different concentrations of ADF/cofilin. *Mol Cell* **24:** 13–23

Applewhite DA, Barzik M, Kojima SI, Svitkina TM, Gertler FB, Borisy GG (2007) Ena/VASP proteins have an anti-capping independent function in filopodia formation. *Mol Biol Cell* **18:** 2579–2591

Carlier MF, Pantaloni D (2007) Control of actin assembly dynamics in cell motility. *J Biol Chem* **282:** 23005–23009

Carlier MF, Ressad F, Pantaloni D (1999) Control of actin dynamics in cell motility. Role of ADF/cofilin. *J Biol Chem* **274:** 33827–33830

Cosen-Binker LI, Kapus A (2006) Cortactin: the gray eminence of the cytoskeleton. *Physiology (Bethesda)* **21:** 352–361

Danuser G, Waterman-Storer CM (2006) Quantitative fluorescent speckle microscopy of cytoskeleton dynamics. *Annu Rev Biophys Biomol Struct* **35:** 361–387

Disanza A, Steffen A, Hertzog M, Frittoli E, Rottner K, Scita G (2005) Actin polymerization machinery: the finish line of signaling networks, the starting point of cellular movement. *Cell Mol Life Sci* **62:** 955–970

Gautreau A, Ho HY, Li J, Steen H, Gygi SP, Kirschner MW (2004) Purification and architecture of the ubiquitous Wave complex. *Proc Natl Acad Sci USA* **101:** 4379–4383

Ghosh M, Song X, Mouneimne G, Sidani M, Lawrence DS, Condeelis JS (2004) Cofilin promotes actin polymerization and defines the direction of cell motility. *Science* **304:** 743–746

Goley ED, Welch MD (2006) The ARP2/3 complex: an actin nucleator comes of age. *Nat Rev Mol Cell Biol* **7:** 713–726

Goode BL, Eck MJ (2007) Mechanism and function of formins in control of actin assembly. *Annu Rev Biochem* **76:** 593–627

Hahne P, Sechi A, Benesch S, Small JV (2001) Scar/WAVE is localised at the tips of protruding lamellipodia in living cells. *FEBS Lett* **492:** 215–220

Hotulainen P, Paunola E, Vartiainen MK, Lappalainen P (2005) Actin-depolymerizing factor and cofilin-1 play overlapping roles in promoting rapid F-actin depolymerization in mammalian non-muscle cells. *Mol Biol Cell* **16:** 649–664

Iwasa JH, Mullins RD (2007) Spatial and temporal relationships between actin-filament nucleation, capping, and disassembly. *Curr Biol* **17:** 395–406

Kiuchi T, Ohashi K, Kurita S, Mizuno K (2007) Cofilin promotes stimulus-induced lamellipodium formation by generating an abundant supply of actin monomers. *J Cell Biol* **177:** 465–476

Kunda P, Craig G, Dominguez V, Baum B (2003) Abi, Sra1, and Kette control the stability and localization of SCAR/WAVE to regulate the formation of actin-based protrusions. *Curr Biol* **13:** 1867–1875

Loisel TP, Boujemaa R, Pantaloni D, Carlier MF (1999) Reconstitution of actin-based motility of Listeria and Shigella using pure proteins. *Nature* **401:** 613–616

Machesky LM, Atkinson SJ, Ampe C, Vandekerckhove J, Pollard TD (1994) Purification of a cortical complex containing two unconventional actins from Acanthamoeba by affinity chromatography on profilin-agarose. *J Cell Biol* **127:** 107–115

Machesky LM, Insall RH (1998) Scar1 and the related Wiskott–Aldrich syndrome protein, WASP, regulate the actin cytoskeleton through the Arp2/3 complex. *Curr Biol* **8:** 1347–1356

Mejillano MR, Kojima S, Applewhite DA, Gertler FB, Svitkina TM, Borisy GG (2004) Lamellipodial versus filopodial mode of the actin nanomachinery: pivotal role of the filament barbed end. *Cell* **118:** 363–373

Miyoshi T, Tsuji T, Higashida C, Hertzog M, Fujita A, Narumiya S, Scita G, Watanabe N (2006) Actin turnover-dependent fast dissociation of capping protein in the dendritic nucleation actin network: evidence of frequent filament severing. *J Cell Biol* **175:** 947–955

Mullins RD, Heuser JA, Pollard TD (1998) The interaction of Arp2/3 complex with actin: nucleation, high affinity pointed end capping, and formation of branching networks of filaments. *Proc Natl Acad Sci USA* **95:** 6181–6186

Nakagawa H, Terasaki AG, Suzuki H, Ohashi K, Miyamoto S (2006) Short-term retention of actin filament binding proteins on lamellipodial actin bundles. *FEBS Lett* **580:** 3223–3228

Pollard TD (2007) Regulation of actin filament assembly by Arp2/3 complex and formins. *Annu Rev Biophys Biomol Struct* **36:** 451–477

Pollard TD, Borisy GG (2003) Cellular motility driven by assembly and disassembly of actin filaments. *Cell* **112:** 453–465

Quinlan ME, Heuser JE, Kerkhoff E, Mullins RD (2005) *Drosophila* Spire is an actin nucleation factor. *Nature* **433:** 382–388

Raftopoulou M, Hall A (2004) Cell migration: Rho GTPases lead the way. *Dev Biol* **265:** 23–32

Romero S, Le Clainche C, Didry D, Egile C, Pantaloni D, Carlier MF (2004) Formin is a processive motor that requires profilin to accelerate actin assembly and associated ATP hydrolysis. *Cell* **119:** 419–429

Rottner K, Behrendt B, Small JV, Wehland J (1999) VASP dynamics during lamellipodia protrusion. *Nat Cell Biol* **1:** 321–322

Rottner K, Kaverina IN, Stradal TEB (2006) Cytoskeleton proteins. In *Cell Biology, A Laboratory Handbook*, Celis JE (ed), Vol. 3, pp 111–119. London: Elsevier Academic Press

Small JV (1995) Getting the actin filaments straight: nucleation-release or treadmilling? *Trends Cell Biol* **5:** 52–55

Small JV, Isenberg G, Celis JE (1978) Polarity of actin at the leading edge of cultured cells. *Nature* **272:** 638–639

Small JV, Stradal T, Vignal E, Rottner K (2002) The lamellipodium: where motility begins. *Trends Cell Biol* **12:** 112–120

Spudich JA, Watt S (1971) The regulation of rabbit skeletal muscle contraction. I. Biochemical studies of the interaction of the tropomyosin–troponin complex with actin and the proteolytic fragments of myosin. *J Biol Chem* **246:** 4866–4871

Steffen A, Faix J, Resch GP, Linkner J, Wehland J, Small JV, Rottner K, Stradal TE (2006) Filopodia formation in the absence of functional WAVE- and Arp2/3-complexes. *Mol Biol Cell* **17:** 2581–2591

Steffen A, Rottner K, Ehinger J, Innocenti M, Scita G, Wehland J, Stradal TE (2004) Sra-1 and Nap1 link Rac to actin assembly driving lamellipodia formation. *EMBO J* **23:** 749–759

Stradal T, Courtney KD, Rottner K, Hahne P, Small JV, Pendergast AM (2001) The Abl interactor proteins localize to sites of actin polymerization at the tips of lamellipodia and filopodia. *Curr Biol* **11:** 891–895

Stradal TE, Rottner K, Disanza A, Confalonieri S, Innocenti M, Scita G (2004) Regulation of actin dynamics by WASP and WAVE family proteins. *Trends Cell Biol* **14:** 303–311

Stradal TE, Scita G (2006) Protein complexes regulating Arp2/3-mediated actin assembly. *Curr Opin Cell Biol* **18:** 4–10

Tani K, Sato S, Sukezane T, Kojima H, Hirose H, Hanafusa H, Shishido T (2003) Abl interactor 1 promotes tyrosine 296 phosphorylation of mammalian enabled (Mena) by c-Abl kinase. *J Biol Chem* **278:** 21685–21692

Theriot JA, Mitchison TJ (1991) Actin microfilament dynamics in locomoting cells. *Nature* **352:** 126–131

van Rheenen J, Song X, van Roosmalen W, Cammer M, Chen X, Desmarais V, Yip SC, Backer JM, Eddy RJ, Condeelis JS (2007) EGF-induced PIP2 hydrolysis releases and activates cofilin locally in carcinoma cells. *J Cell Biol* **179:** 1247–1259

Wang YL (1985) Exchange of actin subunits at the leading edge of living fibroblasts: possible role of treadmilling. *J Cell Biol* **101:** 597–602

Watanabe N, Mitchison TJ (2002) Single-molecule speckle analysis of actin filament turnover in lamellipodia. *Science* **295:** 1083–1086

Weiner OD, Marganski WA, Wu LF, Altschuler SJ, Kirschner MW (2007) An actin-based wave generator organizes cell motility. *PLoS Biol* **5:** e221

Welch MD, DePace AH, Verma S, Iwamatsu A, Mitchison TJ (1997) The human Arp2/3 complex is composed of evolutionarily conserved subunits and is localized to cellular regions of dynamic actin filament assembly. *J Cell Biol* **138:** 375–384

Wiesner S, Helfer E, Didry D, Ducouret G, Lafuma F, Carlier MF, Pantaloni D (2003) A biomimetic motility assay provides insight into the mechanism of actin-based motility. *J Cell Biol* **160:** 387–398

Woychik RP, Maas RL, Zeller R, Vogt TF, Leder P (1990) 'Formins': proteins deduced from the alternative transcripts of the limb deformity gene. *Nature* **346:** 850–853

Zhu J, Yu D, Zeng XC, Zhou K, Zhan X (2007) Receptor-mediated endocytosis involves tyrosine phosphorylation of cortactin. *J Biol Chem* **282:** 16086–16094

Zicha D, Dobbie IM, Holt MR, Monypenny J, Soong DY, Gray C, Dunn GA (2003) Rapid actin transport during cell protrusion. *Science* **300:** 142–145